Importin a3 regulates chronic pain pathways in peripheral sensory neurons

Importin α3 regulates chronic pain pathways in peripheral sensory neurons

Letizia Marvaldi 1, Nicolas Panayotis 1, Stefanie Alber # 1, Shachar Y Dagan # 1, Nataliya Okladnikov 1, Indrek Koppel 1, Agostina Di Pizio 1, Didi-Andreas Song 1, Yarden Tzur 1, Marco Terenzio 1 2, Ida Rishal 1, Dalia Gordon 1, Franziska Rother 3 4, Enno Hartmann 4, Michael Bader 3 4 5, Mike Fainzilber 6

1Department of Biomolecular Sciences, Weizmann Institute of Science, Rehovot 76100, Israel.

2Molecular Neuroscience Unit, Okinawa Institute of Science and Technology, Kunigami-gun, Okinawa 904-0412, Japan.

3Max Delbrück Center for Molecular Medicine, 13125 Berlin, Germany.

4Center for Structural and Cellular Biology in Medicine, Institute of Biology, University of Lübeck, 23538 Lübeck, Germany.

5Charité - Universitätsmedizin Berlin, 10117 Berlin, Germany.

6Department of Biomolecular Sciences, Weizmann Institute of Science, Rehovot 76100, Israel. mike.fainzilber@weizmann.ac.il.

#Contributed equally.

Abstract

How is neuropathic pain regulated in peripheral sensory neurons? Importins are key regulators of nucleocytoplasmic transport. In this study, we found that importin α3 (also known as karyopherin subunit alpha 4) can control pain responsiveness in peripheral sensory neurons in mice. Importin α3 knockout or sensory neuron–specific knockdown in mice reduced responsiveness to diverse noxious stimuli and increased tolerance to neuropathic pain. Importin α3–bound c-Fos and importin α3–deficient neurons were impaired in c-Fos nuclear import. Knockdown or dominant-negative inhibition of c-Fos or c-Jun in sensory neurons reduced neuropathic pain. In silico screens identified drugs that mimic importin α3 deficiency. These drugs attenuated neuropathic pain and reduced c-Fos nuclear localization. Thus, perturbing c-Fos nuclear import by importin α3 in peripheral neurons can promote analgesia.

The importin α subfamily of karyopherins is critical for nuclear import in eukaryotic cells (1, 2) and participates in cytoplasmic transport in large cells such as neurons (3, 4). Despite overlapping importin specificities (5, 6), differential expression profiles and varying cargo affinities enable regulation of specific functions by single importins (7–15). We sought to identify neuronal functions of importins by behavioral screens on importin α knockout mice.

We corroborated these findings by intrathecal injection of adeno-associated virus 9 (AAV9) constructs for acute knockdown or overexpression of importin α3 (fig. S2). Importin α3 knockdown mice revealed delayed paw withdrawal latency to noxious heat in comparison with mice that received control short hairpin RNA (shRNA) (Fig. 1BOpens in image viewer), without any significant effects on exploratory behavior or motor coordination (fig. S3, A and B). Specificity of the effects was confirmed by reversal of the phenotype upon importin α3 overexpression in importin α3 knockout mice (Fig. 1COpens in image viewer). Conversely, shRNA knockdown had no further effect in the knockout background (fig. S3C). Thus, specific loss of importin α3 attenuates responsiveness to diverse noxious stimuli.

We next evaluated importin α3 in neuropathic pain using the spared nerve injury (SNI) model (16–18) (fig. S4, A and B), with periodic monitoring of mechanosensitivity in wild-type and importin α3 SNI animals over 3 months. Initial responses were similar in both genotypes and diverged from day 60 onward. At this later stage, importin α3 null animals exhibited increasing tolerance to SNI, with less hypersensitivity to touch (Fig. 1DOpens in image viewer) and reduced unevoked paw clenching (fig. S4C), whereas wild-type animals did not show any improvement. Similar results were obtained by knockdown of importin α3 before induction of SNI (Fig. 1EOpens in image viewer and fig. S4, D and E). Starting 60 days after injury, control shRNA-treated SNI mice typically displayed a spontaneous clenched-paw phenotype associated with reduced paw print width in the CatWalk assay, while animals treated with anti–importin α3 shRNA revealed improved gait parameters and reduced paw clenching (fig. S4, E and F). Mechanosensitivity assays showed that the neuropathic pain response developed in a similar manner in control and anti–importin α3 shRNA treated mice up to 60 days after injury. From day 60 onward, importin α3 knockdown animals exhibited a significant recovery of the paw withdrawal reflex, in contrast to controls (Fig. 1EOpens in image viewer). Thus, both knockout and acute knockdown of importin α3 provides relief from chronic neuropathic pain in the SNI model.

Different cell types can participate in neuropathic pain circuits (19, 20). We therefore sought to determine whether importin α3 effects on neuropathic pain arise specifically in sensory neurons. To this end, we carried out viral transduction of shRNA using AAV-PHP.S, a capsid subtype developed for peripheral neuron specificity (21). We verified AAV-PHP.S selectivity by lumbar intrathecal injection, observing specific and efficient transduction of dorsal root ganglia (DRG) sensory neurons (fig. S5). We then tested the effects of importin α3 knockdown by AAV-PHP.S delivery of shRNA after SNI induction (fig. S4D), monitoring both evoked (Fig. 1FOpens in image viewer) and unevoked (Fig. 1GOpens in image viewer, fig. S4G, and movie S1) responses to neuropathic pain. Both the evoked and spontaneous parameters revealed that sensory neuron–specific knockdown of importin α3 provided relief from neuropathic pain, even when knockdown was initiated after establishment of the pain model.

To gain mechanistic insight on the effects of importin α3 knockout in SNI, we compared DRG transcriptomes at 1 week versus 11 weeks after injury, when pain was significantly alleviated (Fig. 2AOpens in image viewer and table S1). The differentially expressed gene sets revealed signatures for a number of transcription factors affected by depletion of importin α3 (Fig. 2BOpens in image viewer). Among these factors, the activator protein 1 (AP1) family was prioritized for further study because c-Fos is a well-documented marker for pain circuits (22–

24). Quantitative analysis of four AP1 target genes after SNI revealed reduced expression of Syngap1 and RTL1 in importin α3 null DRG compared with wild type (Fig. 2COpens in image viewer). Syngap1 has previously been implicated in tactile sensory processing (25).

c-Fos features both an importin α–binding nuclear localization signal and a binding motif for transportin, a distinct nuclear import factor (26). Multiple members of both these nuclear import factor families are widely expressed in sensory neurons (27). We confirmed importin α3 and c-Fos expression in DRG neurons (fig. S6, A to C) and verified that they interact by proximity biotinylation in transfected Neuro2a (N2a) cells (fig. S6D) and proximity ligation assay (PLA) of endogenous proteins in sensory neurons (Fig. 2, D and EOpens in image viewer). Basal c-Fos expression was not changed in importin α3 knockout neurons (fig. S6, E and F). c-Fos immunostaining was mostly nuclear in wild-type DRG neurons, whereas, in contrast, there was little or no c-Fos nuclear accumulation in importin α3 null neurons (Fig. 2, F to IOpens in image viewer, and fig. S6, A, B, and G). Thus, importin α3 is required for c-Fos nuclear accumulation in adult sensory neurons.

The c-Fos inhibitor T-5224 is under investigation for analgesic efficacy (28, 29). We tested the effects of T-5224 by intraperitoneal injection in wild-type versus importin α3 null mice. T-5224 treatment increased paw withdrawal latency in response to noxious heat in wild-type mice (fig. S7, A to D), but it had no additional effect beyond the already existing attenuation in importin α3 null animals (fig. S7, C and D). However, T-5224 did ameliorate the paw withdrawal latency in von Frey tests of wild-type animals 1 week after induction of SNI (fig. S7E), a time point at which importin α3 knockout or knockdown still had no effect on SNI responses (Fig. 1Opens in image viewer). Thus c-Fos perturbation has analgesic effects, and importin α3 may act mainly in the later maintenance stage of neuropathic pain.

To confirm that the AP1 pathway is required for late-stage neuropathic pain, we tested the effects of c-Fos or c-Jun knockdown in the SNI model (fig. S8). Similarly to the effects of importin α3 depletion, c-Fos knockdown reduced sensitivity to noxious heat (Fig. 3AOpens in image viewer) without affecting basal mechanosensitivity (Fig. 3BOpens in image viewer). c-Jun knockdown reduced sensitivity to both noxious heat and mechanical stimuli (Fig. 3, A and BOpens in image viewer). Comparison of c-Fos, c-Jun, and importin α3 knockdowns in the SNI model showed that all three shRNAs significantly attenuated the neuropathic pain response 67 to 90 days after injury (Fig. 3COpens in image viewer). Furthermore, neuron-specific expression of a dominant-negative form of AP1 called A-Fos (30) significantly attenuated noxious heat sensitivity without affecting basal mechanosensitivity (Fig. 3, D and EOpens in image viewer) and significantly reduced late-stage neuropathic pain in SNI (Fig. 3FOpens in image viewer). Thus, AP1 pathway inhibition attenuates neuropathic pain in the SNI model.

Finally, we carried out an in silico screen using the Connectivity Map (CMap) database (31, 32) to search for drugs that might target the importin α3–c-Fos pathway. The screen identified ~50 compounds with high CMap scores, 35 of which were not known to affect pain (Fig. 4AOpens in image viewer and table S2). We selected three compounds for further analysis: ajmaline, an antiarrhythmic alkaloid; sulmazole, a cardiotonic agent; and sulfamethizole, an antibiotic. Ajmaline did not affect responses to noxious heat, but both sulmazole and sulfamethizole

showed efficacy in this assay (Fig. 4BOpens in image viewer). Both of the latter drugs also provided time- and dose-dependent relief at both early and late stages of SNI (Fig. 4, C to EOpens in image viewer, and fig. S9, A and B) and were as effective as knockout or knockdown of importin α3 in ameliorating response of SNI animals to a noxious mechanical stimulus (Fig. 4FOpens in image viewer). Additionally, both sulmazole and sulfamethizole significantly reduced c-Fos nuclear accumulation in wild-type neurons but did not have any further effect on c-Fos nuclear accumulation in importin α3 null neurons (fig. S9, C to E). Thus, drugs mimicking importin α3 loss phenocopy both the analgesic and c-Fos localization effects observed in importin α3 mutant animals.

Here, we have shown that perturbing c-Fos nuclear import by importin α3 in sensory neurons reduces sensitivity to noxious stimuli and provides analgesia specifically in the maintenance phase of neuropathic pain. Direct c-Fos inhibition is effective at both early and maintenance stages of neuropathic pain, suggesting that other modes of c-Fos nuclear import or other transcription factors may control the early pain response, while importin α3 has a key role for later chronic pain. Very recent studies have reported discrimination at the spinal circuit level between rapid aversive behavior and sustained pain responses (33), as well as roles for different cell types in mechanosensitivity and nociception (19, 20). Our findings indicate that peripheral sensory neurons are the locus of the effects of importin α3 on sustained neuropathic pain. The expression profiles and levels of both importin α3 and c-Fos are conserved between mouse and human DRG (34), and a recent study reported marked up-regulation of AP1 family genes in the DRG of neuropathic pain patients (35), highlighting the potential of importin α3 as a drug target for pain. Chronic pain is currently one of the most common unmet medical needs, owing to limited analgesic efficacy of existing drugs, coupled with adverse side effects (36, 37). Moreover, opioids, which are the most commonly used class of pain drugs, carry multiple risks of tolerance and dependence, which can lead to considerable levels of abuse (38). The vast majority of current targets for drug development in the pain field are ion channels and neurotransmitter receptors, localized at the plasma membrane and the synapse. Importin α3 provides an alternative target both in terms of molecular identity and subcellular localization, offering opportunities for future analgesia development.

Acknowledgments

We thank V. Kiss, T. Shalit, M. Tsoory, and C. Pritz for excellent professional expertise; N. Korem and Y. Levi for technical assistance; and H. Song, C. Vinson, and V. Gradinaru for generous gifts of essential plasmids via Addgene. Funding: Supported by research grants from the European Research Council (Advanced grant Neurogrowth, Proof of Concept grant ChronicPain), the Irwin Green Alzheimer's Research Fund, the Simon Family Foundation, and Mr. and Mrs. Lawrence Feis. N.P., I.K., and M.T. were partly supported by Koshland senior postdoctoral fellowships, and N.P. was also supported by the Israeli Ministry of Immigrant Absorption. M.F. is supported by the Chaya Professorial Chair in Molecular Neuroscience at the Weizmann Institute of Science. Author contributions: Conceptualization: M.F. and L.M.; behavior and pain models: L.M., N.P., S.Y.D., N.O., and S.A.; immunohistochemistry, biochemistry, and data analyses: L.M., N.P., S.A., I.K., A.D.P., D.-A.S., Y.T., M.T., I.R., and D.G.; mouse models: F.R., E.H., and M.B.; writing and revision: M.F. and L.M., with input from all

authors; supervision and funding: M.F. Competing interests: L.M. and M.F. have patent applications related to this work [Israeli application 268111, pending; Patent Cooperation Treaty (PCT) PCT/IL2020/050801]. Data and materials availability: All data are available in the main text or the supplementary materials. RNA sequencing datasets are available in the GEO database online (accession no. GSE137515). The importin α3 null mouse model is available upon request from M.B.'s laboratory.

REFERENCES AND NOTES

1. Y. Miyamoto, K. Yamada, Y. Yoneda, J. Biochem. 160, 69–75 (2016).

2. M. Christie et al., J. Mol. Biol. 428, 2060–2090 (2016).

3. N. Panayotis, A. Karpova, M. R. Kreutz, M. Fainzilber,

Trends Neurosci. 38, 108–116 (2015).

4. M. Terenzio, G. Schiavo, M. Fainzilber, Neuron 96, 667–679 (2017).

5. B. Friedrich, C. Quensel, T. Sommer, E. Hartmann, M. Köhler,

Mol. Cell. Biol. 26, 8697–8709 (2006).

6. M. T. Mackmull et al., Mol. Syst. Biol. 13, 962 (2017).

7. T. Shmidt et al., Nat. Cell Biol. 9, 1337–1338 (2007).

8. F. Rother et al., PLOS ONE 6, e18310 (2011).

9. G. Gabriel et al., Nat. Commun. 2, 156 (2011).

10. T. Moriyama et al., FEBS J. 278, 1561–1572 (2011).

11. K. Ben-Yaakov et al., EMBO J. 31, 1350–1363 (2012).

12. N. Yasuhara et al., Dev. Cell 26, 123–135 (2013).

13. N. Panayotis et al., Cell Rep. 25, 3169–3179.e7 (2018).

14. A. S. Sowa et al., Proc. Natl. Acad. Sci. U.S.A. 115,

E2624–E2633 (2018).

15. K. Döhner et al., PLOS Pathog. 14, e1006823 (2018).

16. I. Decosterd, C. J. Woolf, Pain 87, 149–158 (2000).

17. M. Pertin, R. D. Gosselin, I. Decosterd, Methods Mol. Biol. 851,

205–212 (2012).

18. S. Shiers et al., J. Neurosci. 38, 7337–7350 (2018).

19. H. Abdo et al., Science 365, 695–699 (2019).

20. X. Yu et al., Nat. Commun. 11, 264 (2020).

21. K. Y. Chan et al., Nat. Neurosci. 20, 1172–1179 (2017).
22. R. E. Coggeshall, Prog. Neurobiol. 77, 299–352 (2005).
23. P. L. Santos, R. G. Brito, J. P. S. C. F. Matos, J. S. S. Quintans,
L. J. Quintans-Júnior, Mol. Neurobiol. 55, 4560–4579 (2018).
24. J. Lai et al., Nat. Neurosci. 9, 1534–1540 (2006).
25. S. D. Michaelson et al., Nat. Neurosci. 21, 1–13 (2018).
26. M. Arnold, A. Nath, D. Wohlwend, R. H. Kehlenbach,
J. Biol. Chem. 281, 5492–5499 (2006).
27. N. Sharma et al., Nature 577, 392–398 (2020).
28. Y. Aikawa et al., Nat. Biotechnol. 26, 817–823 (2008).
29. H. Makino et al., Sci. Rep. 7, 16983 (2017).
30. M. Olive et al., J. Biol. Chem. 272, 18586–18594 (1997).
31. J. Lamb et al., Science 313, 1929–1935 (2006).
32. A. J. Mears et al., NPJ Genom. Med. 2, 14 (2017).
33. T. Huang et al., Nature 565, 86–90 (2019).
34. P. Ray et al., Pain 159, 1325–1345 (2018).
35. R. Y. North et al., Brain 142, 1215–1226 (2019).
36. A. S. Yekkirala, D. P. Roberson, B. P. Bean, C. J. Woolf,
Nat. Rev. Drug Discov. 16, 545–564 (2017).
37. T. J. Price et al., Nat. Rev. Neurosci. 19, 383–384 (2018).
38. P. Skolnick, N. D. Volkow, Neuron 92, 294–297 (2016).

ACKNOWLEDGMENTS

We thank V. Kiss, T. Shalit, M. Tsoory, and C. Pritz for excellent professional expertise; N. Korem and Y. Levi for technical assistance; and H. Song, C. Vinson, and V. Gradinaru for generous gifts of essential plasmids via Addgene. Funding: Supported by research grants from the European Research Council (Advanced grant Neurogrowth, Proof of Concept grant ChronicPain), the Irwin Green Alzheimer's Research Fund, the Simon Family Foundation, and Mr. and Mrs. Lawrence Feis. N.P., I.K., and M.T. were partly supported by Koshland senior

postdoctoral fellowships, and N.P. was also supported by the Israeli Ministry of Immigrant Absorption. M.F. is supported by the Chaya Professorial Chair in Molecular Neuroscience at the Weizmann Institute of Science. Author contributions: Conceptualization: M.F. and L.M.; behavior and pain models: L.M., N.P., S.Y.D., N.O., and S.A.; immunohistochemistry, biochemistry, and data analyses: L.M., N.P., S.A., I.K., A.D.P., D.-A.S., Y.T., M.T., I.R., and D.G.; mouse models: F.R., E.H., and M.B.; writing and revision: M.F. and L.M., with input from all authors; supervision and funding: M.F. Competing interests: L.M. and M.F. have patent applications related to this work [Israeli application 268111, pending; Patent Cooperation Treaty (PCT) PCT/IL2020/050801]. Data and materials availability: All data are available in the main text or the supplementary materials. RNA sequencing datasets are available in the GEO database online (accession no. GSE137515). The importin a3 null mouse model is available upon request from M.B.'s laboratory.

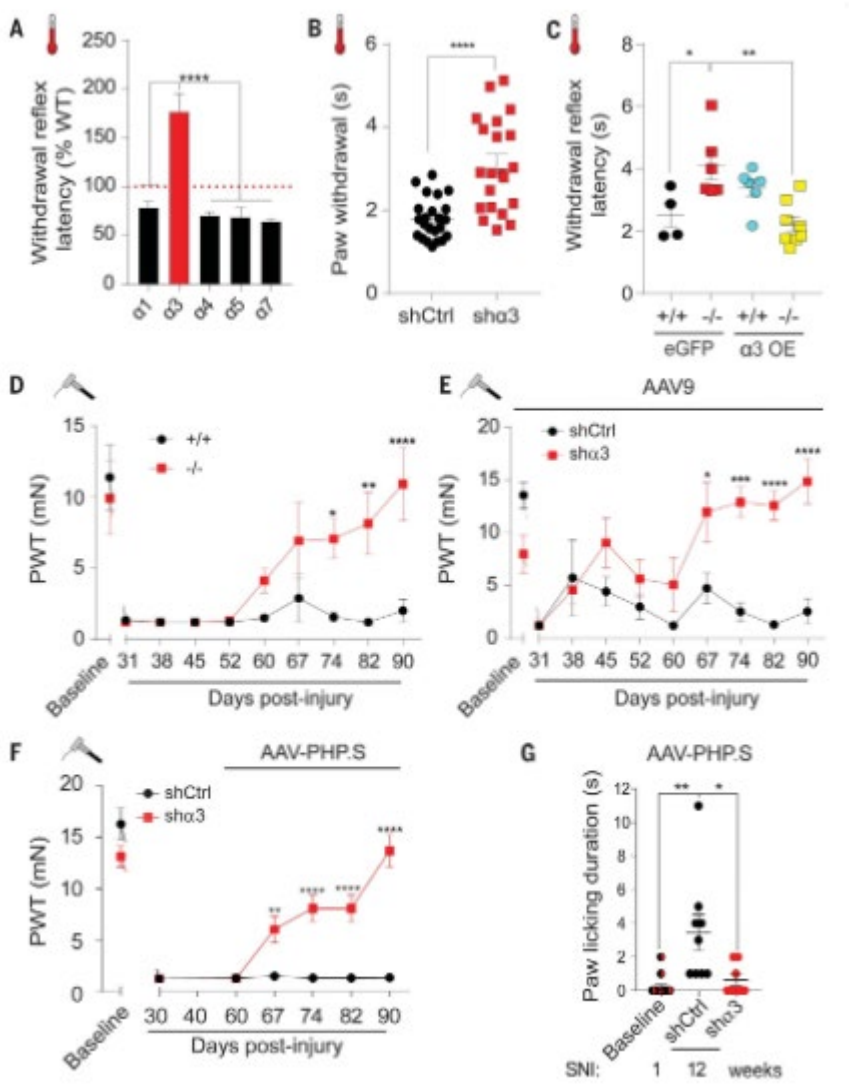

Fig. 1. Attenuated pain responses in importin a3 mice. (A) Importin a3 mice (a3) are the only line of importin a knockout mice with a higher latency of paw withdrawal in response to noxious heat stimulus (58°C) compared with wild-type littermates. n ≥ 7 mice, one-way analysis of variance (ANOVA) followed by Tukey's multiple comparison test. (B) Attenuated response to noxious heat after shRNA-mediated knockdown of importin a3. n = 20 mice, two-tailed unpaired t test. (C) Overexpression

of importin a3 (a3 OE) restored heat sensitivity in importin a3 knockout animals, while enhanced green fluorescent protein (eGFP) overexpression had no such effect. n ≥ 4 mice, one-way ANOVA followed by Tukey's multiple comparison test. (D) Paw withdrawal threshold (PWT) assessed by the von Frey test in SNI animals shows alleviation of long-term neuropathic pain in importin a3 knockout animals. n ≥ 5 mice, two-way ANOVA followed by Sidak's multiple comparison test. (E) PWT in SNI animals treated with AAV9 shRNA against importin a3 (sha3) or scrambled control shRNA (shCtrl). The upper horizontal line indicates time frame from AAV9 injection. n = 7 mice, two-way ANOVA followed by Sidak's multiple comparison test. (F) PWT in SNI animals treated with AAV-PHP.S shRNA against importin a3 (sha3) or shCtrl. The upper horizontal line indicates time frame from AAV-PHP.S injection. n = 9 mice, two-way ANOVA followed by Sidak's multiple comparison test. (G) Spontaneous (unevoked) paw licking duration measured at 1 week (baseline) and 12 weeks after SNI. n ≥ 9 mice per group, Kruskal-Wallis followed by Dunn's multiple comparison tests. All quantifications shown as mean ± SEM. *P < 0.05, **P < 0.01, ***P < 0.001, ****P < 0.0001.

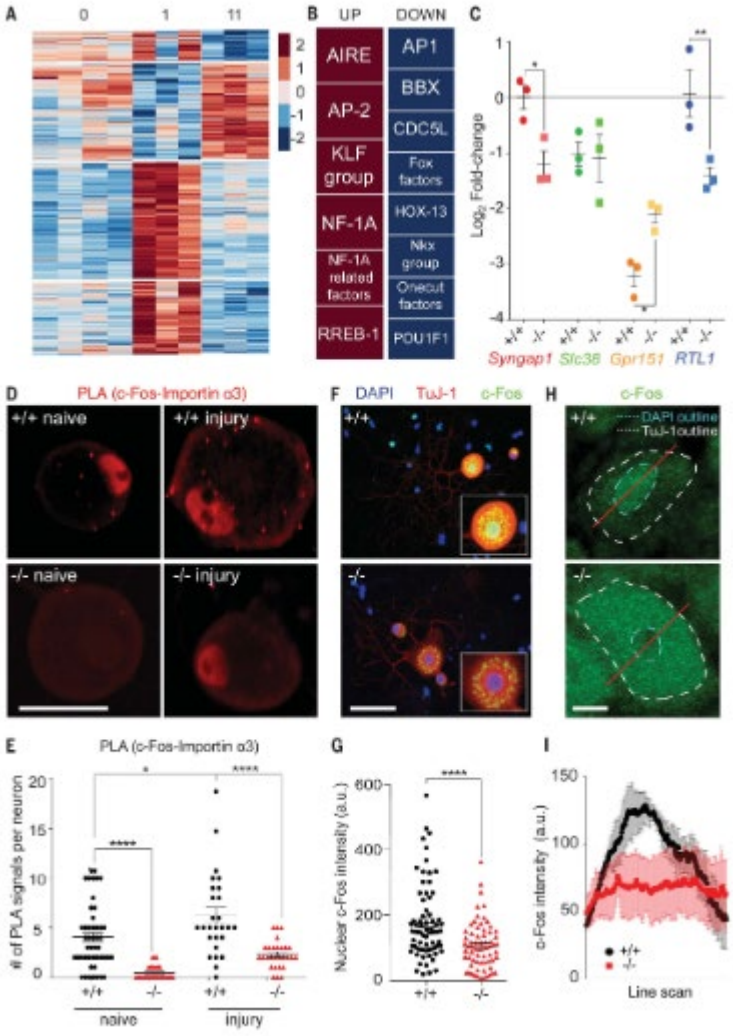

Fig. 2. Transcriptome analyses suggest that c-Fos nuclear import by importin a3 mediates pain responses. (A) Heatmap of z-score transformed normalized expression values for 530 differentially expressed genes (DEG) at the indicated times (weeks) after SNI in importin a3 null mice (n ≥ 3 mice). (B) FMatch (geneXplain) TRANSFAC analyses identify transcription factor (TF) families enriched in DEG pro-

moters from the up-regulated (161) and down-regulated (369) genes at 11 weeks after SNI. The AP1 complex was identified as one of the top TF families for the down-regulated gene ensemble. (C) Reverse transcription quantitative polymerase chain reaction (RT-qPCR) analysis of four AP1-target genes, Syngap1, Slc38, Gpr151, and RTL1, comparing expression at 1 week versus 11 weeks after SNI in wild-type and importin a3 null DRGs. n = 3 mice, one-way ANOVA followed by Sidak's multiple comparison test. (D) Proximity ligation assay (PLA) for c-Fos and importin a3 in calcitonin gene-related peptide–positive DRG neurons fixed after 24 hours in culture from both naïve and injury groups. PLA signals shown in red. Scale bar, 30 mm. (E) Quantification of PLA signals per neuron. n ≥ 29 neurons per group from three independent experiments, ANOVA followed by Tukey's multiple comparison test. (F) Reduced nuclear localization of c-Fos in cultured importin a3 null DRG neurons versus wild type. Scale bar, 50 mm. (G) Quantification of nuclear c-Fos

intensity from the experiment shown in (F). n > 67 neurons from three independent experiments, two-tailed unpaired t test. (H) Reduced nuclear localization of c-Fos in DRG neurons from sectioned ganglia of importin a3 null compared with wild-type mice. Cell body and nucleus boundaries determined by TuJ-1 and 4',6-diamidino-2-phenylindole (DAPI) staining as indicated (see also fig. S6G). Scale bar, 10 mm. (I) Quantification of c-Fos immunofluorescence along line scans as shown in (H), n > 206 neurons from three independent experiments. All data are shown as mean ± SEM. a.u., arbitrary units. *P < 0.05, **P < 0.01, ****P < 0.0001.

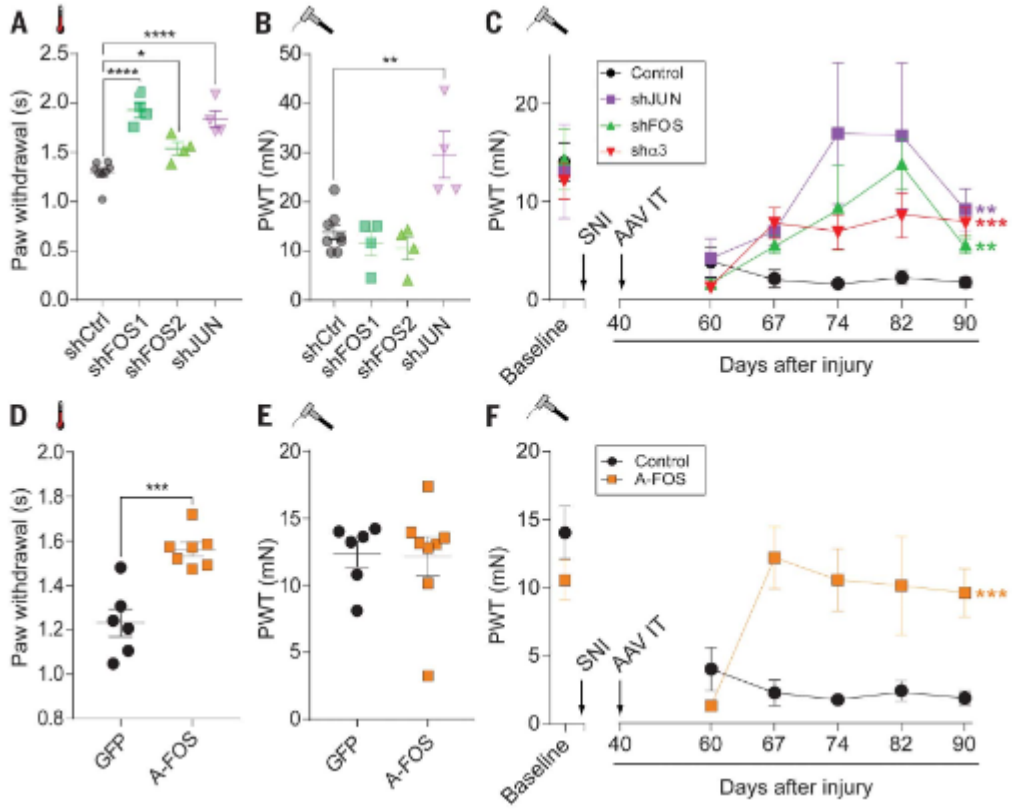

Fig. 3. Acute knockdown or dominant-negative inhibition of AP1 transcription factors attenuates chronic pain after SNI. (A) Reduced noxious heat responses in mice after intrathecal AAV9 delivery of shRNAs targeting c-Fos (shFOS1, shFOS2) or c-Jun (shJUN). n ≥ 4 mice, ANOVA followed by Dunnett's multiple comparison test. (B) Reduced mechanosensitivity in shJUN, but not shFOS, treated animals. n ≥ 4 mice, ANOVA followed by Dunnett's multiple comparison test. (C) PWT assessed by the von Frey test in SNI animals treated with the indicated shRNAs (shFOS indicates a mixture of both). n ≥ 5 mice, two-way ANOVA. AAV IT, adeno-associated virus intrathecal injection. (D and E) AAV9 overexpression of the A-Fos

dominant-negative (DN) under the neuron-specific human synapsin I promoter reduces noxious heat responses (D) without effects on basal mechanosensitivity (E). n ≥ 6 mice, two-tailed unpaired t test. (F) PWT in SNI animals treated with the A-Fos DN construct. n ≥ 6 mice, two-way ANOVA. Asterisks indicate significant treatment effects between the groups. All data shown as mean ± SEM. *P < 0.05, **P < 0.01, ***P < 0.001, ****P < 0.0001.

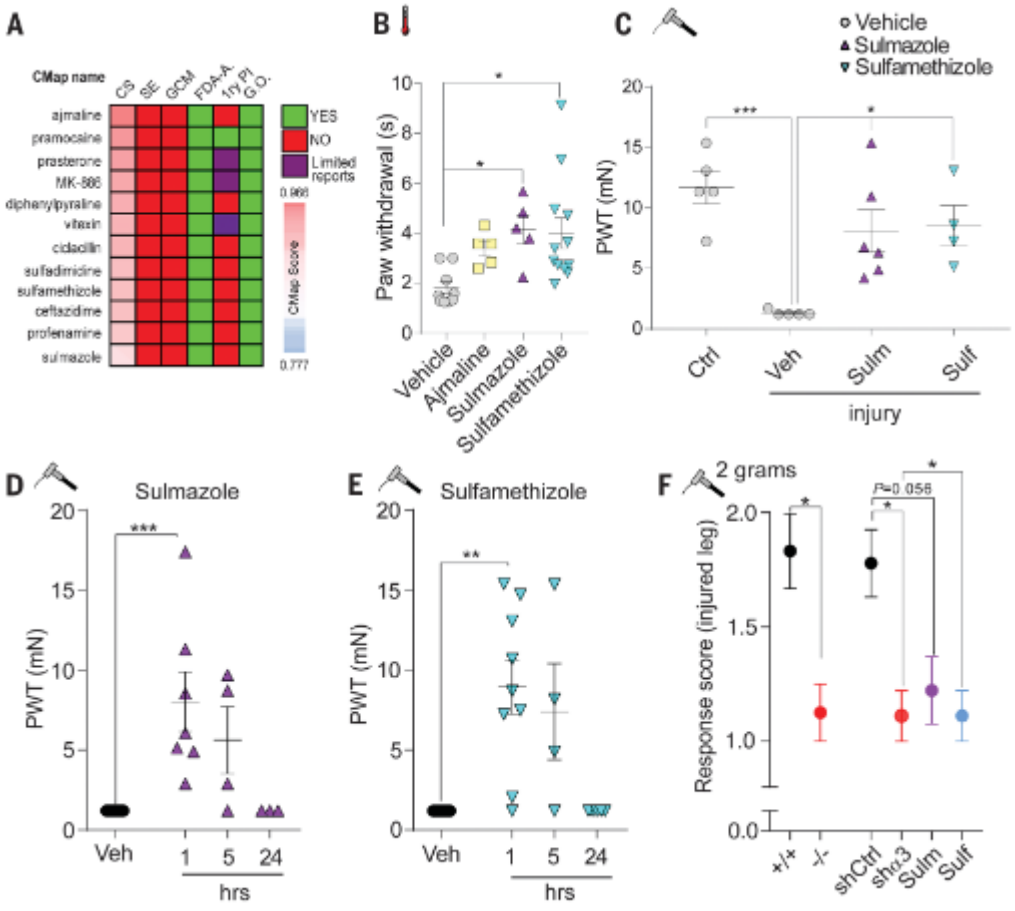

Fig. 4. An in silico screen for mimics of transcriptional effects of importin a3 loss reveals candidate analgesics. (A) Impa3 knockout DEG

lists were used to query CMap for small molecules with similar effects on cell line transcriptomes. Compounds with CMap scores (CS) > 0.85 are shown. Compounds were further filtered for minimal predicted side effects (SE), lack of general cell-modifying effects (GCM), U.S. Food and Drug Administration approved status (FDA-A), whether their primary therapeutic indication (PI) is pain-related, and final go/no-go decision (G.O., general observation). (B) Three candidates meeting the desired criteria were tested in vivo for effects on response to noxious heat 1 hour after intraperitoneal injection. Sulmazole (0.5 mg/kg, n = 5 mice) and sulfamethizole (1.25 mg/kg, n = 12) showed significant effects as compared with vehicle [5% dimethyl sulfoxide (DMSO) in phosphate-buffered saline (PBS), n = 9 mice], while ajmaline (1 mg/kg, n = 5 mice) did not. (C) Significant effects of sulmazole (1.25 mg/kg, n = 6 mice) and sulfamethizole (3.12 mg/kg, n = 4 mice) compared with vehicle (5% DMSO in PBS, n = 5 mice) in the SNI model of neuropathic pain. Drugs were tested 60 days after establishing the model by two intraperitoneal injections 1 week apart, followed by von Frey tests 1 hour after the second injection. Ctrl, control (i.e., the uninjured leg); Veh, vehicle; Sulm, sulmazole; Sulf, sulfamethizole. ANOVA followed by Sidak's multiple comparison test used for both (B) and (C). (D and E) Duration of drug effects 1 week after SNI, with von Frey tests performed 1, 5, and 24 hours after intraperitoneal injection. n ≥ 4 mice, Kruskal-Wallis test followed by Dunn's multiple comparison test. (F) Noxious mechanosensitivity testing of SNI mice treated as

shown, using von Frey filaments of 2 gram-force. Scoring from 0 to 2, with 0 indicating no response, 1 indicating signs of discomfort, and 2 indicating withdrawal of the

leg. n ≥ 6 mice, Kruskal-Wallis test followed by Dunn's multiple comparison test. Data shown as mean ± SEM throughout. *P < 0.05, **P < 0.01, ***P < 0.001.